9950-153

DRL No. 135
Technical Report: MRI - 292

DOE/JPL - 955676-83
Distribution Category UC - 63

ANALYSIS OF DEFECT STRUCTURE IN SILICON

EFFECT OF GRAIN BOUNDARY DENSITY ON CARRIER MOBILITY IN UCP MATERIAL

Silicon Sheet Growth Development for the Large Area Silicon Sheet Task of the Low-Cost Solar Array Project.

INTERIM REPORT

by
J. Dunn
G. B. Stringfellow
R. Natesh

November, 1982

JPL Contract No. 955676

The JPL Low-Cost Silicon Solar Array Project is sponsored by the U.S. Department of Energy and forms part of the Solar Photovoltaic Conversion Program to initiate a major effort toward the development of low-cost solar arrays. This work was performed for the Jet Propulsion Laboratory, California Institute of Technology, by agreement between NASA and DOE.

MRI Materials Research, Inc.

Research
Development
Consulting and Testing
Of Materials

700 South 790 East
Centerville, Utah 84014
Telephone (801) 298-4000

DRL No. 135
Technical Report: MRI - 292

DOE/JPL - 955676-1
Distribution Category UC - 63

ANALYSIS OF DEFECT STRUCTURE IN SILICON

EFFECT OF GRAIN BOUNDARY DENSITY ON CARRIER MOBILITY IN UCP MATERIAL

**Silicon Sheet Growth Development
for the Large Area Silicon Sheet Task of
the Low-Cost Solar Array Project.**

INTERIM REPORT

by
J. Dunn
G. B. Stringfellow
R. Natesh

November, 1982

JPL Contract No. 955676

The JPL Low-Cost Silicon Solar Array Project is sponsored by the U.S. Department of Energy and forms part of the Solar Photovoltaic Conversion Program to initiate a major effort toward the development of low-cost solar arrays. This work was performed for the Jet Propulsion Laboratory, California Institute of Technology, by agreement between NASA and DOE.

MRI Materials Research, Inc.

Research
Development
Consulting and Testing
Of Materials

700 South 790 East
Centerville, Utah 84014
Telephone: (801) 298-4000

TECHNICAL CONTENT STATEMENT

This report was prepared as an account of work sponsored by the United States Government. Neither the United States nor the United States Department of Energy, nor any of their employees, nor any of their contractors, subcontractors, or their employees, make any warranty, express or implied, or assumes any legal liability or responsibility for the accuracy, completeness, or usefulness of any information, apparatus, product, or process disclosed, or represents that its use would not infringe privately-owned rights.

CONTENTS

LIST OF FIGURES

LIST OF TABLES

SECTION I

ABSTRACT

A study was made to determine the relationships between hole mobility and grain boundary density. Mobility was measured using the van der Pauw technique, and grain boundary density was measured using a quantitative microscopy technique. Mobility was found to decrease with increasing grain boundary density.

SECTION II

INTRODUCTION

The objective of this work is to determine the relationship between carrier mobility and grain boundary density, that is grain boundary length per unit area, in cast polycrystalline silicon.

A polycrystalline wafer sliced from a cast mold will have many defects ranging from vacancies to precipitates, twins, dislocations, and grain boundaries. When considering the effect on carrier mobility, grain boundaries are thought to have the greatest influence.[1]

There are several reasons that grain boundaries are considered the limiting factor in mobilities. The most obvious is the high concentration of other defects at a boundary. Since there is a lattice mismatch at a boundary, there is bound to be a high vacancy density. These vacancies act as a sink for dopant atoms, thus resulting in an ionized impurity concentration near the boundary that is higher than the rest of the crystal matrix. Sirce ionized impurities act as scattering centers for charge carriers, mobilities will necessarily be lowered.

Another feature of a grain boundary is band bending. That is to say the conduction and valence bonds, at the grain boundary, are bent up and down respectively thus presenting an energy barrier for electrons and holes. This, too, should decrease mobility.

Carrier mobility was measured via the Hall effect [2-9] using a four-point-probe configuration. Important parameters such as resistivity, carrier type, and carrier concentration were also measured. Grain boundary density was measured by quantitative optical microscopy [10].

SECTION III

EXPERIMENTAL PROCEDURE

Equipment List

Kiethly instruments model 225 current source
Hewlett Packard 412 A vacuum tube voltmeter
Kiethly instruments model 600 B electrometer
Harvey Wells model 1050A magnet power supply
Magnion 7" electromagnet
Power Logicon model 5C ultrasonic wire bonder
Nikon Optiphot optical microscope
Olympus OSM optical microscope
Hewlett Packard 3465 A Multi meter

Eight (8) SEMIX samples from UCP Ingot 5848-13 C were used in this study. These samples were designated by JPL as A-13, B-2, C-12, D-8, E-13, F-2, G-12, and H-8. The samples were first characterized for structural defects as described in an earlier report [10]. The specimens for Hall mobility measurements were obtained from each of the above 8 samples by scribing a line parallel to one of the edges,and then cleaving the sample along the scribed line. The cleaved piece was then broken into three smaller pieces. Therefore, initially there were 24 irregular specimens of sizes ranging from 2mm by 5mm to 5mm by 5mm. Due to breakage and handling problems only 20 specimens were eventually characterized. Thickness was measured by placing

samples on edge and measuring them with a filar eyepiece at a magnification of about X100 with the Olympus microscope.

Electrical connections were made by mounting the sample on a PC board with four copper strips then, using an ultrasonic wire bonder, 18μm aluminum wire was bonded to the silicon surface and then to the copper strip (Fig. 1). This technique was used so that the contact area would be as small as possible and be bonded as close to the edge of silicon sample as possible so as to reduce the influence of the contacts on the measurements. The power and time settings for the silicon and copper bonds were 2 and 1.6, and 2.4 and 2 respectively.

Resistivity measurements were made using the configurations in Fig. 2. Current was passed through the contacts depicted in the figure and the corresponding potential induced at the other contacts was measured. This procedure was repeated in both configurations, with the current flowing in the forward and reverse directions and at .1 and 1mA to insure ohmic behavior in that region. The ammeter insures that the desired current is indeed what is flowing between the points in question.

Hall voltages were measured with the electrical connections in the configurations shown in Fig. 3. Current was passed through the contacts shown in each configuration and the potential across the other contacts was measured. The magnetic field, which is perpendicular to the face of the sample, was then applied. The voltage was then measured again. The difference between the two readings is the hall voltage. The procedure was repeated in both configurations with the current flowing in the forward and reverse directions. The sample was

then turned around 180 degrees with respect to the magnetic field and the procedure was carried out again. This procedure negates the effects of any physical assymmetries in the experimental setup. Most of the samples were measured with a current of 1ma and an 8KG magnetic field. Some samples were run at different levels of current and magnetic field to facilitate more accurate voltage readings.

Grain boundary density was determined by examining the samples at 400X with the Nikon microscope. The diameter of the field of vision was determined with a calibrated microscope slide. The number of grain boundaries that intersected the circumference of the field of vision were then counted. Due to the irregular shapes and sizes of the samples the number of fields of vision per sample varied greatly. To preserve some statistical validity a grid was used to determine where to locate the center of a given field. See Fig. 4 for a portion of the grid. Each dot represents the center of a field of vision and there is 0.5mm between dots on a horizontal row.

SECTION IV

RESULTS AND SAMPLE CALCULATIONS

Thickness

The calibration of the filar eyepiece on the Olympus microscope when using the 10X objective is 0.9909 μm/div . Data taken for the three pieces from sample G-12 is shown in Table 1. Final results for all eight samples is shown in Table 2.

TABLE 1

THICKNESS MEASUREMENTS ON SAMPLE G-12

	INITIAL READING	FINAL READING	d(div)	d(μm)
1	276	564	288	265
2	361	653	292	289
3	208	526	318	315

d = 296μm max. % deviation = 6.4%

TABLE 2

THICKNESS DATA FOR ALL SAMPLES

sample	d(μm)	max.% deviation
A - 13	266	2.4
B - 2	315	3.1
C - 12	304	1.2
D - 8	277	5.5
E - 13	305	3.5
F - 2	290	0.8
G - 12	296	6.4
H - 8	285	1.7

Resistivity

Using the configurations (1) and (2) in Fig. 2, the resistances R_{ABCD} and R_{BCDA}, respectively, can be measured where

$$R_{ABCD} = \frac{\text{Potential across DC}}{\text{Current through AB}} = \frac{V_{DC}}{I_{AB}}$$

and

$$R_{BCDA} = \frac{\text{Potential across DA}}{\text{Current through BC}} = \frac{V_{DA}}{I_{BC}}$$

It was shown by Van der Pauw[11] that the following relation holds:

$$\exp\left[-\pi R_{ABCD}\left(\frac{d}{\rho}\right)\right] + \exp\left[-\pi R_{DCBA}\left(\frac{d}{\rho}\right)\right] = 1 \qquad \textit{equation (1)}$$

where d is the sample thickness and ρ is the resistivity of the sample. Since the resistances and thickness of a given sample are known, ρ can be determined by use of equation (1).

A calculation of ρ for the first of the C-12 samples, C-12-1, follows:

C-12-1

$$I = 1\text{mA} \qquad R_{ABCD} = \frac{.00145 + .0015}{2I} = 1.47\ \Omega$$

$$R_{BCDA} = \frac{.045 + .045}{2I} = 45\ \Omega$$

$$I = 100\mu\text{A} \qquad R_{ABCD} = \frac{.00015 + .00015}{2I} = 1.5\ \Omega$$

$$R_{BCDA} = \frac{.0045 + .0046}{2I} = 45.5\ \Omega$$

$\bar{R}_{ABCD} = 1.485$ ohm, $\bar{R}_{BCDA} = 45.25$ ohm; using these values and $d = 304\mu\text{m}$, equation (1) gives $\rho = 1.8\Omega\text{-cm}$.

Hall const., Mobility, Carrier conc., and Carrier Type

The Hall const., mobility, carrier conc., and carrier type were determined using the configurations shown in Fig. 3. Data taken for sample G-12-2 is shown in Table 3. This is followed by sample calculations.

Sample:G-12-2

I = 1mA, B = 8KG, d = 296μm, ρ = 2.1Ω-cm

TABLE 3

MEASURED VOLTAGES ON SAMPLE G-12-2

	Configuration 1			Configuration 2		
	V_1(B=0)	V_2(B≠0)	V_H	V_1(B=0)	V_2(B≠0)	V_H
+I +B	.05	.0515	.0015	.056	.055	.001
−I +B	.056	.057	.001	.052	.051	.001
+I −B	.056	.055	.001	.052	.053	.001
−I −B	.051	.05	.001	.056	.057	.001

$\overline{V_1 - V_2} = \bar{V}_H = .0011V$

$$\text{Hall const.} \equiv R_H = \frac{\bar{V}_H d}{BI} = \frac{(.0011V)(296 \times 10^{-4}cm)}{10^{-3}amps\ 8.5\times10^{-5}w/cm^2} = 393cm^3/coul$$

$$\text{Hall mobility} \equiv \mu_H = \frac{R_H}{\rho} = \frac{393}{2.1} = 187cm^2/v\text{-}sec$$

$$\text{Carrier conc.} \equiv P = \frac{1}{R_H q} = \frac{1}{393(1.6 \times 10^{-19}coul)} = 1.58 \times 10^{16}cm^{-3}$$

where q = charge of an electron.

Carrier type is determined by the following example:

> if V_1 is >0 when $B = 0$, there is an excess of negative charge near the contact D (ref. Fig. 5), when $B \neq 0$ and $V_2 > V_1$ the charge carrier is a hole since it travels in the direction of conventional current and is deflected by a force, $\vec{F} = q(\vec{V} \times \vec{B})$ thereby increasing the positive potential between B and D.

Normalized Mobilities

Hole mobility may be given by the relation:[12]

$$\mu^P = \mu_{min} + \frac{\mu_{max} - \mu_{min}}{1 + \left(\frac{P}{P_{ref}}\right)^{\alpha}}$$

where $\mu_{min} = 47.7\ cm^2/v\text{-}sec$

$\mu_{max} = 495\ cm^2/v\text{-}sec$

$P_{ref} = 6.3 \times 10^{16}\ cm^{-3}$

and

$\alpha = .76$

The hole mobility normalized to a carrier conc. of $P = 10^{16} cm^{-3}$, μ^*, is given by

$$\mu^* = \mu_H \left(\frac{\mu^{10^{16}}}{\mu^P}\right)$$

where μ_H is the hall mobility, and $\mu^{10^{16}} = 406\ cm^2/v\text{-}sec$.

Grain Boundary Density

The grain boundary density, G.B., is calculated by using the following relation from Brandon[13]:

$$G.B. = \left(\frac{\pi}{2}\right)\left(\frac{P_L}{N}\right) cm/cm^2$$

$$\text{where } P_L = \frac{\text{total number of intersections of grain boundaries with the test line}}{\text{unit length of the test line}}$$

and N = No. of fields of vision.

At 400X the diameter of the field of vision is .043 cm so the circumference, length of the test line, is $(\pi)(.043)$ cm.

A calculation of G.B. for sample D-8-1 follows:

D-8-1

$$P_L = 50 \qquad N = 59$$

$$G.B. = \left(\frac{\pi}{2}\right)\frac{50}{\pi(.043)\,59} = 9.85 \text{ cm/cm}^2$$

A summary of results is listed in Table 4. This table lists data for resistivity, Hall mobility, carrier concentration, hole mobility, normalized hole mobility, and grain boundary density for all 20 specimens.

TABLE 4

Resistivity, Hall Mobility, Carrier Concentration, Hole Mobility, Normalized Hole Mobility, and Grain Boundary Density for All 20 Specimens

SAMPLE	$\rho\Omega$-cm)	μ_H(cm^2/v-sec)	P x 10^{16}(cm^{-3})	μ^P(cm^2/v-sec)	$\frac{\mu^{10^{16}}}{\mu^P}$	μ^* cm^2/v-s	G.B.(cm/cm^2)
A-1	1.65	201	1.80	370	1.10	221	4.42
B-1	2.45	176	1.44	385	1.05	185	9.06
B-2	3.00	213	.97	408	1.00	213	16.97
B-3	1.85	212	1.58	379	1.07	227	12.41
C-1	1.80	337	1.02	405	1.00	337	2.12
C-2	1.69	198	1.86	368	1.10	218	15.17
C-3	2.20	187	1.51	382	1.06	198	11.86
D-1	2.20	178	1.59	378	1.07	190	9.85
D-2	2.15	177	1.64	376	1.08	191	6.43
D-3	3.10	85	2.36	351	1.16	99	16.16
E-1	1.86	274	1.26	393	1.03	282	0
E-2	1.75	226	1.58	379	1.07	242	.32
F-1	2.30	199	1.36	388	1.05	209	15.23
F-2	2.60	104	2.30	353	1.15	120	20.46
F-3	2.15	242	1.15	399	1.02	247	15.61
G-1	2.05	240	1.26	393	1.03	247	10.00
G-2	2.10	187	1.58	379	1.07	200	12.79
H-1	1.50	380	1.09	402	1.01	384	2.52
H-2	1.55	124	2.00	363	1.12	139	13.25
H-3	1.58	202	1.90	366	1.10	224	18.45

SECTION V

DISCUSSIONS

When hole mobility is plotted as a function of grain boundary density a trend develops. That is, mobility decreased as a function of grain boundary density. This result, based on the electronic features of grain boundaries, is expected. But, it must be noted that while there is a clear trend, there is no clearly defined fundamental relationship evident.

It is noted that for grain boundary densities above all but the lowest values, the great majority of samples have mobility values centered near 200 cm^2/v-sec for raw data (Fig. 6) and 215 cm^2/v-sec for the normalized data (Fig. 7). It is also noted that within this region there is no defined trend between mobility and grain boundary density. Several explanations may be offered to explain this behavior.

It may be proposed that the range of grain boundary density is too small to allow conclusions to be drawn concerning a cause and effect relationship. Perhaps grain boundary densities spanning several orders of magnitude should be examined to determine if a fundamental relationship can be observed.

It may be reasoned that ~200 cm^2/v-sec is the "characteristic" mobility for all but the most defect free samples. Those samples with much lower values are vastly different in the nature of their defect structure. One such difference may be the precipitate density. A precipitate will act as a scattering center and so it stands to reason that a sample with an extremely large precipitate density would have lower mobility

values than would be expected based on grain boundary density alone.

Another factor that is likely to affect the mobility as a function of grain boundary density is the grain size distribution and the geometric distribution of grain boundaries on the samples themselves. Distances between grain boundaries ranged from ~100μm to more than a millimeter. There is no clearly defined relationship between mobility and grain sizes nor is there enough sample area available to get a statistically valid idea of the grain size distribution.

Geometric considerations must also be examined. That is to say, what is the actual distribution of grain boundaries on the sample. Grain boundary density does not take into account the uniformity of boundary distribution. It is reasonable to assume that two samples, one with grain boundaries uniformly distributed and the other with nearly all its boundaries concentrated in one portion of the sample, will have different mobility characteristics even if the grain boundary density is the same for both. Since there is no quantitative method to analyze and relate the "boundary distribution" to boundary density, ambiguous results are likely if boundary density is considered the only independent parameter.

SECTION VI

CONCLUSIONS

Mobility measurements were made on twenty SEMIX samples using the van der Pauw technique. Grain boundary density was measured using a quantitative microscopy technique.

The mobility was found to decrease with increasing boundary density. Although an obvious trend appeared in the data, no fundamental relationship could be determined.

Possible causes for the lack of a fundamental relationship are as follows:

1) Insufficient range of data with respect to grain boundary densities.

2) In some cases scattering mechanisms other than grain boundaries may limit mobility, such as precipitates, dislocations, and twin boundaries.

3) Nonuniformity of grain size and geometric distribution may lead to ambiguous results.

It is proposed that MRI generate quantitative information to establish a fundamental relationship between mobility and grain boundary density.

SECTION VII

REFERENCES

1. J. Y. M. Lee and I. C. Cheng, J. Appl. Phys., vol. 53, p. 490, 1982.

2. R. A. Smith, "Semiconductors," Cambridge University Press, London, 1959.

3. E. H. Putley, "The Hall Effect and Semiconductor Physics", Butterworth and Co. (Publishers), Ltd., London, 1960: Dover Publications, Inc., New York, 1968.

4. A. C. Beer, "Galvanomagnetic Effects in Semiconductors", Academic Press, Inc., New York, 1963.

5. L. P. Hunter, Phys. Rev., vol. 94, p. 1157 - 1160, 1954.

6. L. P. Hunter, E. Hulbregtse, and R. Anderson, Phys. Rev., vol. 91, p. 1315 - 1320, 1953.

7. G. L. Pearson and J. Bardeen, Phys. Rev., vol. 75, p. 865 - 883, 1949.

8. K. Pigon, J. Appl. Phys., vol. 32, p. 2369 - 2371, 1961.

9. R. L. Petritz, Phys. Rev., vol. 110, p. 1254 - 1262, 1958.

10. R. Natesh, T. Guyer, and G. B. Stringfellow, "Analysis of Defect Structure in Silicon: Characterization of Samples from UCP Ingot 5848 - 13C", Interim Report, Technical Report: MRI - 290, Materials Research, Inc., August, 1982.

11. L. J. van der Pauw, Phillips Research Reports, vol. 13, p. 1, 1958.

12. R. S. Muller and T. I. Kamins, "Device Electronics for Integrated Circuits," (New York: Wiley 1977) p. 26.

13. D. G. Brandon, "Modern Techniques in Metallography," (Princeton, N. J. : D. van Nostrand Company 1966) p. 241.

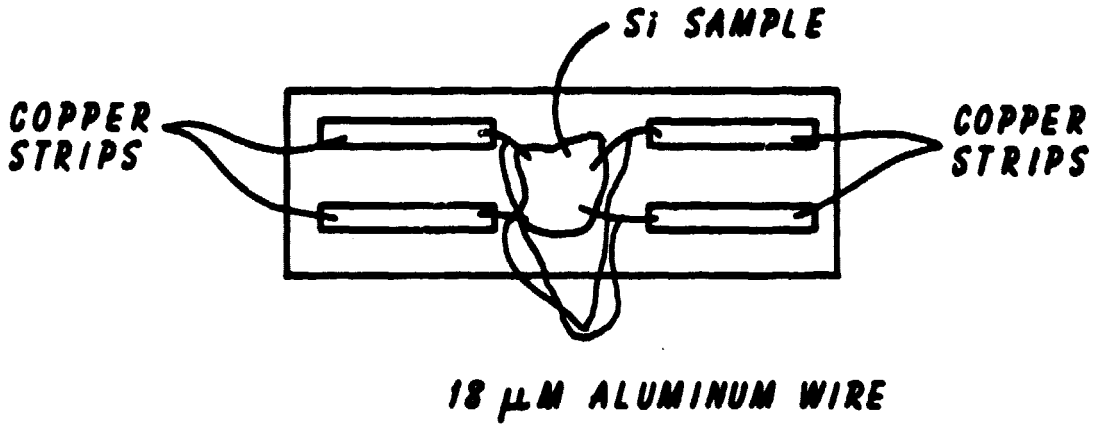

Fig. 1 Electrical Connections to Obtain a Small Contact Area and Reduce Contact Influence on Measurements

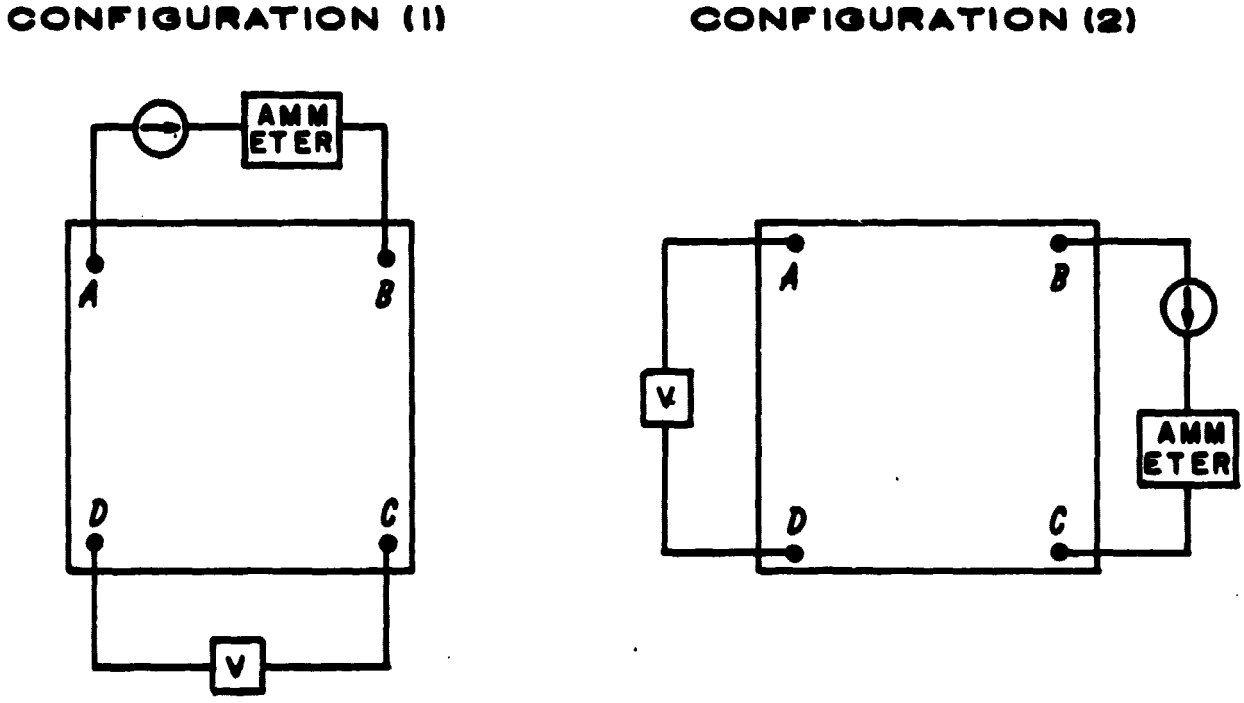

Fig. 2 Two Types of Configurations Used for Resistivity Measurements

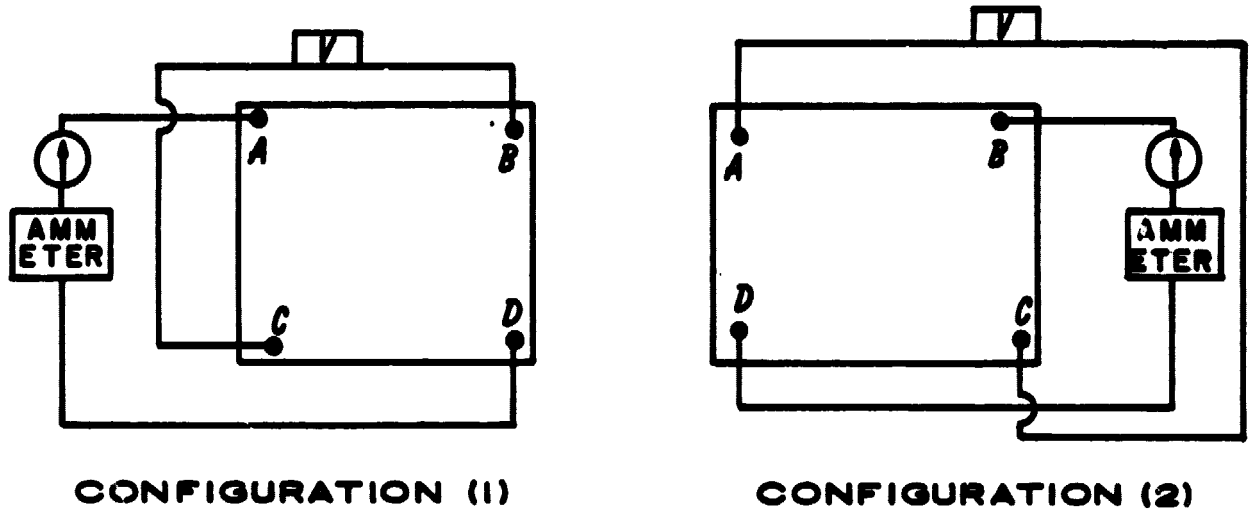

Fig. 3 Two Types of Configurations Used for Hall Voltage Measurements

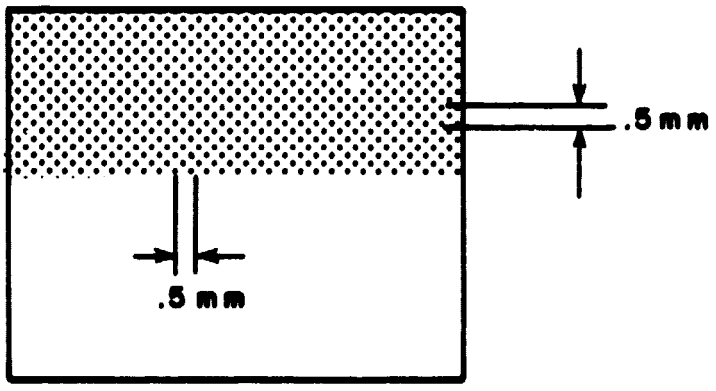

Fig. 4 Grid Used to Locate the Center of a Given Field

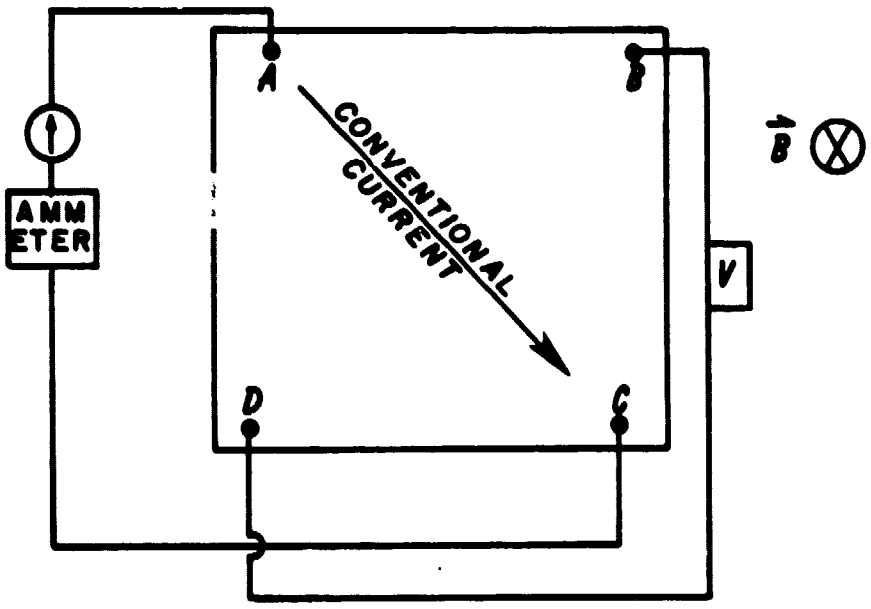

Fig. 5 Configuration Used to Determine Carrier Type

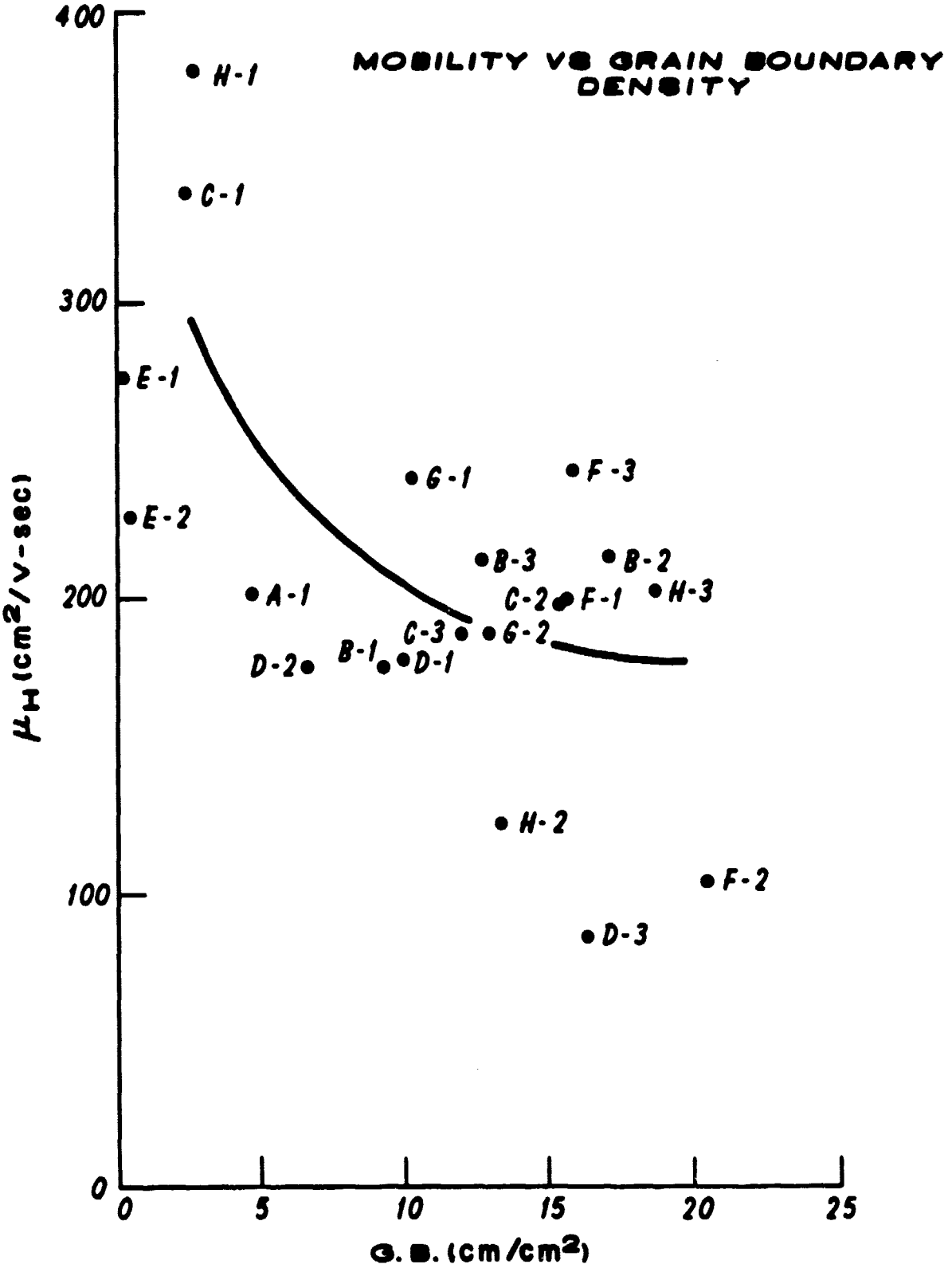

Fig. 6 Relationship Between Mobility and Grain Boundary Density

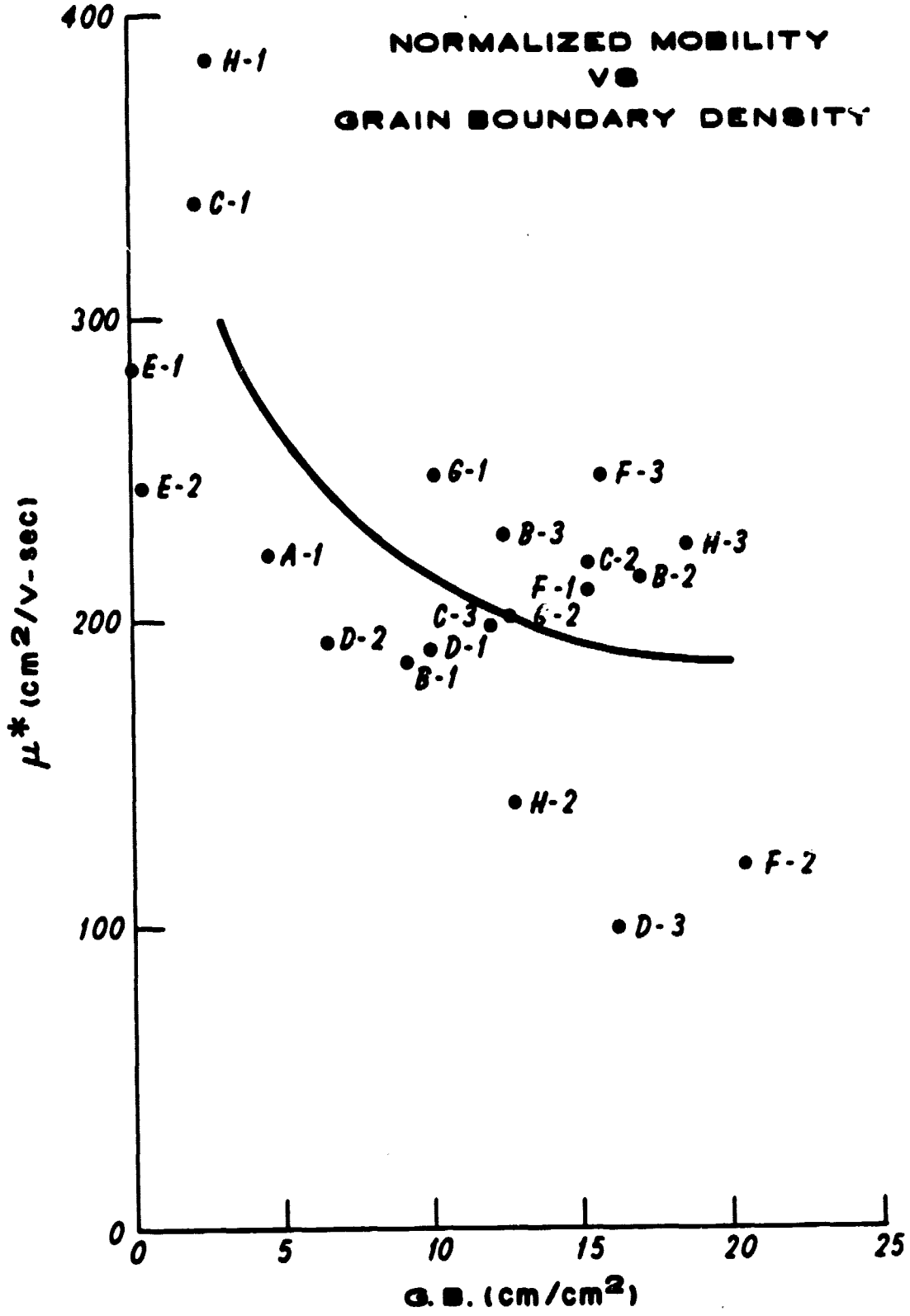

Fig. 7 Relationship Between Normalized Mobility and Grain Boundary